

University of Nebraska - Lincoln

DigitalCommons@University of Nebraska - Lincoln

Kenneth Bloom Publications

Research Papers in Physics and Astronomy

11-1-1997

New upper limit on the decay $\eta \rightarrow e^+ e^-$

T. E. Browder

University of Hawaii at Manoa, Honolulu, Hawaii

Kenneth A. Bloom

University of Nebraska-Lincoln, kenbloom@unl.edu

CLEO Collaboration

Follow this and additional works at: <https://digitalcommons.unl.edu/physicsbloom>



Part of the [Physics Commons](#)

Browder, T. E.; Bloom, Kenneth A.; and Collaboration, CLEO, "New upper limit on the decay $\eta \rightarrow e^+ e^-$ " (1997). *Kenneth Bloom Publications*. 158.

<https://digitalcommons.unl.edu/physicsbloom/158>

This Article is brought to you for free and open access by the Research Papers in Physics and Astronomy at DigitalCommons@University of Nebraska - Lincoln. It has been accepted for inclusion in Kenneth Bloom Publications by an authorized administrator of DigitalCommons@University of Nebraska - Lincoln.

New upper limit on the decay $\eta \rightarrow e^+ e^-$

T. E. Browder, F. Li, Y. Li, and J. L. Rodriguez
University of Hawaii at Manoa, Honolulu, Hawaii 96822

T. Bergfeld, B. I. Eisenstein, J. Ernst, G. E. Gladding, G. D. Gollin, R. M. Hans, E. Johnson, I. Karliner, M. A. Marsh,
M. Palmer, M. Selen, and J. J. Thaler
University of Illinois, Champaign-Urbana, Illinois 61801

K. W. Edwards
Carleton University, Ottawa, Ontario, Canada K1S 5B6
and the Institute of Particle Physics, Canada

A. Bellerive, R. Janicek, D. B. MacFarlane, K. W. McLean, and P. M. Patel
McGill University, Montréal, Québec, Canada H3A 2T8
and the Institute of Particle Physics, Canada

A. J. Sadoff
Ithaca College, Ithaca, New York 14850

R. Ammar, P. Baringer, A. Bean, D. Besson, D. Copping, C. Darling, R. Davis, N. Hancock, S. Kotov,
I. Kravchenko, and N. Kwak
University of Kansas, Lawrence, Kansas 66045

S. Anderson, Y. Kubota, M. Lattery, S. J. Lee, J. J. O'Neill, S. Patton, R. Poling, T. Riehle, V. Savinov, and A. Smith
University of Minnesota, Minneapolis, Minnesota 55455

M. S. Alam, S. B. Athar, Z. Ling, A. H. Mahmood, H. Severini, S. Timm, and F. Wappler
State University of New York at Albany, Albany, New York 12222

A. Anastassov, S. Blinov,^{*} J. E. Duboscq, K. D. Fisher, D. Fujino,[†] K. K. Gan, T. Hart, K. Honscheid, H. Kagan, R. Kass,
J. Lee, M. B. Spencer, M. Sung, A. Undrus,^{*} R. Wanke, A. Wolf, and M. M. Zoeller
Ohio State University, Columbus, Ohio 43210

B. Nemati, S. J. Richichi, W. R. Ross, and P. Skubic
University of Oklahoma, Norman, Oklahoma 73019

M. Bishai, J. Fast, E. Gerndt, J. W. Hinson, N. Menon, D. H. Miller, E. I. Shibata, I. P. J. Shipsey, and M. Yurko
Purdue University, West Lafayette, Indiana 47907

L. Gibbons, S. Glenn, S. D. Johnson, Y. Kwon, S. Roberts, and E. H. Thorndike
University of Rochester, Rochester, New York 14627

C. P. Jessop, K. Lingel, H. Marsiske, M. L. Perl, D. Ugolini, R. Wang, and X. Zhou
Stanford Linear Accelerator Center, Stanford University, Stanford, California 94309

T. E. Coan, V. Fadeyev, I. Korolkov, Y. Maravin, I. Narsky, V. Shelkov, J. Staeck, R. Stroynowski,
I. Volobouev, and J. Ye
Southern Methodist University, Dallas, Texas 75275

M. Artuso, A. Efimov, F. Frascioni, M. Gao, M. Goldberg, D. He, S. Kopp, G. C. Moneti, R. Mountain, S. Schuh,
T. Skwarnicki, S. Stone, G. Viehhauser, and X. Xing
Syracuse University, Syracuse, New York 13244

J. Bartelt, S. E. Csorna, V. Jain, and S. Marka
Vanderbilt University, Nashville, Tennessee 37235

R. Godang, K. Kinoshita, I. C. Lai, P. Pomianowski, and S. Schrenk
Virginia Polytechnic Institute and State University, Blacksburg, Virginia 24061

G. Bonvicini, D. Cinabro, R. Greene, L. P. Perera, and G. J. Zhou
Wayne State University, Detroit, Michigan 48202

B. Barish, M. Chadha, S. Chan, G. Eigen, J. S. Miller, C. O'Grady, M. Schmidtler, J. Urheim,
A. J. Weinstein, and F. Würthwein
California Institute of Technology, Pasadena, California 91125

D. M. Asner, D. W. Bliss, G. Masek, H. P. Paar, S. Prell, M. Sivertz, and V. Sharma
University of California, San Diego, La Jolla, California 92093

J. Gronberg, T. S. Hill, R. Kutschke, D. J. Lange, S. Menary, R. J. Morrison, H. N. Nelson, T. K. Nelson, C. Qiao,
J. D. Richman, D. Roberts, A. Ryd, and M. S. Witherell
University of California, Santa Barbara, California 93106

R. Balest, B. H. Behrens, W. T. Ford, H. Park, J. Roy, and J. G. Smith
University of Colorado, Boulder, Colorado 80309-0390

J. P. Alexander, C. Bebek, B. E. Berger, K. Berkelman, K. Bloom, D. G. Cassel, H. A. Cho, D. M. Coffman,
D. S. Crowcroft, M. Dickson, P. S. Drell, K. M. Ecklund, R. Ehrlich, R. Elia, A. D. Foland, P. Gaidarev, R. S. Galik,
B. Gittelman, S. W. Gray, D. L. Hartill, B. K. Heltsley, P. I. Hopman, J. Kandaswamy, P. C. Kim, D. L. Kreinick, T. Lee,
Y. Liu, G. S. Ludwig, J. Masui, J. Mevisen, N. B. Mistry, C. R. Ng, E. Nordberg, M. Ogg,[‡] J. R. Patterson,
D. Peterson, D. Riley, A. Soffer, B. Valant-Spaight, and C. Ward
Cornell University, Ithaca, New York 14853

M. Athanas, P. Avery, C. D. Jones, M. Lohner, C. Prescott, J. Yelton, and J. Zheng
University of Florida, Gainesville, Florida 32611

G. Brandenburg, R. A. Briere, Y. S. Gao, D. Y.-J. Kim, R. Wilson, and H. Yamamoto
Harvard University, Cambridge, Massachusetts 02138

(CLEO Collaboration)
(Received 3 June 1997)

We have searched for the rare decay of the η meson $\eta \rightarrow e^+ e^-$ using the CLEO II detector. The η 's were produced in $e^+ e^-$ collisions with 10 GeV center-of-mass energy at the Cornell Electron Storage Ring (CESR). We find with 90% confidence the upper limit on the branching fraction $B(\eta \rightarrow e^+ e^-) < 7.7 \times 10^{-5}$. The application of conventional elementary particle theory to this decay predicts a branching fraction of about 10^{-9} . [S0556-2821(97)01421-5]

PACS number(s): 14.40.Aq, 13.40.Hq

I. INTRODUCTION

We have used the CLEO II detector at the Cornell Electron Storage Ring (CESR) to study about 2×10^7 events of the form $e^+ e^- \rightarrow$ hadrons to search for the rare decay mode $\eta \rightarrow e^+ e^-$. We have not found this decay, only a 90% confidence upper limit of $B(\eta \rightarrow e^+ e^-) < 7.7 \times 10^{-5}$. As discussed in Sec. II on the conventional theory of this decay, the predicted branching fraction is about 10^{-9} . An observation of a signal above this level could be evidence for an unconventional process which enhances the $\eta \rightarrow e^+ e^-$ decay rate.

The plan of this paper is as follows. Section II gives the conventional theory for the decay and the predicted relation-

ship between $B(\eta \rightarrow e^+ e^-)$ and the measured branching fraction $B(\eta \rightarrow \mu^+ \mu^-)$. Then Sec. III describes the data and the calculation of the number of η 's produced in the 2×10^7 hadron events. Section IV describes the method used to search for $\eta \rightarrow e^+ e^-$ decays. Finally Sec. V contains the calculation of the upper limit on $B(\eta \rightarrow e^+ e^-)$, a discussion of the errors, and some general remarks on the search.

II. CONVENTIONAL THEORY FOR $\eta \rightarrow e^+ e^-$ AND $\eta \rightarrow \mu^+ \mu^-$

The η is massive enough ($547 \text{ MeV}/c^2$) to decay via $\eta \rightarrow \mu^+ \mu^-$ as well as via $\eta \rightarrow e^+ e^-$. Figure 1 shows the decay mechanism according to conventional theory [1,2]. The decay matrix element for η into two virtual photons, represented by the cross hatched circle, is difficult to calculate from first principles. Indeed the same problem occurs in the study of the decay $\pi^0 \rightarrow e^+ e^-$ [1,2].

Landsberg [2] has reviewed the conventional theory for

*Permanent address: BINP, RU-630090 Novosibirsk, Russia.

[†]Permanent address: Lawrence Livermore National Laboratory, Livermore, CA 94551.

[‡]Permanent address: University of Texas, Austin, TX 78712.

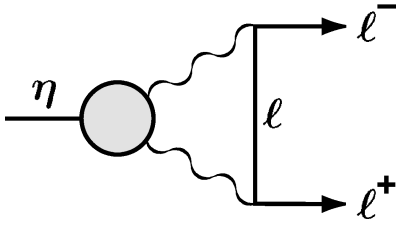


FIG. 1. Feynman diagram for the conventional theory of the decays $\eta \rightarrow e^+ e^-$ and $\eta \rightarrow \mu^+ \mu^-$. l represents an e or a μ .

the decay $P \rightarrow l^+ l^-$ where P is a pseudoscalar meson, and he gives the formula for the branching fraction

$$B(P \rightarrow l^+ l^-) = B(P \rightarrow \gamma\gamma) 2\alpha^2 r^2 s [|X|^2 + |Y|^2]. \quad (1)$$

Here $B(P \rightarrow \gamma\gamma)$ is the branching fraction for $P \rightarrow \gamma\gamma$, α is the fine structure constant, $r = m_l/m_P$ where m_l and m_P are the l and P masses, and $s = (1 - 4r^2)^{1/2}$. Y is proportional to the imaginary part of the decay amplitude and has the explicit form

$$|Y| = \frac{1}{s} \ln \left(\frac{1+s}{2r} \right). \quad (2)$$

X is proportional to the real part of the decay amplitude, and is difficult to calculate with certainty. Of course even if X is calculated precisely, Eq. (1) is still not a basic formula because $B(P \rightarrow \gamma\gamma)$ must be taken from experiment. Nevertheless Eq. (1) with $X=0$ gives a lower limit on $B(P \rightarrow l^+ l^-)$, namely,

$$B(P \rightarrow l^+ l^-) > B(P \rightarrow \gamma\gamma) \frac{2\alpha^2 r^2}{s} \left[\ln \left(\frac{1+s}{2r} \right) \right]^2. \quad (3)$$

Using the $\eta \rightarrow \gamma\gamma$ branching fraction from the Particle Data Group [3],

$$B(\eta \rightarrow \gamma\gamma) = 0.393 \pm 0.003 \quad (4)$$

and Eq. (3) we can calculate

$$B(\eta \rightarrow \mu^+ \mu^-)_{\min} = 4.4 \times 10^{-6}. \quad (5)$$

The measured branching fraction [3–5],

$$B(\eta \rightarrow \mu^+ \mu^-)_{\text{measured}} = (5.7 \pm 0.8) \times 10^{-6}, \quad (6)$$

is consistent with this limit. If we assume that the ratio $|X|^2/|Y|^2$ is the same for $\eta \rightarrow e^+ e^-$ and $\eta \rightarrow \mu^+ \mu^-$ then

$$\frac{B(\eta \rightarrow e^+ e^-)}{B(\eta \rightarrow \mu^+ \mu^-)} = \left(\frac{r_e}{r_\mu} \right)^2 \frac{[\ln[(1+s_e)/2r_e]]^2 s_\mu}{[\ln[(1+s_\mu)/2r_\mu]]^2 s_e}, \quad (7)$$

where the e and μ subscripts refer to m_e and m_μ in $r = m_l/m_P$. The dominant term, $(r_e/r_\mu)^2 = (m_e/m_\mu)^2$, is due to helicity suppression. From Eq. (7),

$$\frac{B(\eta \rightarrow e^+ e^-)}{B(\eta \rightarrow \mu^+ \mu^-)} = 4.05 \times 10^{-4}. \quad (8)$$

Equation (8) also holds for $B(\eta \rightarrow e^+ e^-)_{\min}/B(\eta \rightarrow \mu^+ \mu^-)_{\min}$. Using this and Eq. (5),

$$B(\eta \rightarrow e^+ e^-)_{\min} = 1.8 \times 10^{-9}. \quad (9)$$

Finally, combining Eqs. (6) and (8),

$$B(\eta \rightarrow e^+ e^-) \approx 2.3 \times 10^{-9}. \quad (10)$$

This estimated branching fraction is based on the assumption that $|X|^2/|Y|^2$ is the same for the $e^+ e^-$ and $\mu^+ \mu^-$ decays. An unknown process present in the decay $\eta \rightarrow e^+ e^-$, but not in the decay $\eta \rightarrow \mu^+ \mu^-$, could result in a value of $|X|^2/|Y|^2$ much larger in the $e^+ e^-$ mode, and thus a signal larger than the above limit.

III. DATA AND NUMBER OF η 'S PRODUCED

A. Detector and data

We used data collected by the CLEO II detector [6] at CESR. The components of the detector which are most critical to this study are the three concentric cylindrical drift chambers occupying the space 4 cm to 95 cm radially from the beam axis, comprising a 67-layer charged-particle tracking system which is immersed in a 1.5 T solenoidal magnetic field. The momentum p , in GeV, of charged particles is measured with a resolution of $\sigma_p/p(\%) \approx [(0.15p)^2 + (0.5)^2]^{1/2} \approx 0.5\%$ for the electrons we see in η decay. In addition, ionization loss (dE/dx) is measured in the 51-layer main drift chamber with a resolution of 6–7 %.

Also important for the measurements reported here is an electromagnetic calorimeter consisting of 7800 thallium-doped CsI crystals. These crystals, each of dimension $\sim 5 \text{ cm} \times 5 \text{ cm} \times 30 \text{ cm}$, surround the tracking volume, covering 98 % of the full solid angle. Forming the barrel region of the calorimeter, 6144 tapered crystals are arrayed just inside the magnet coil at a radius of $\sim 1 \text{ m}$ in a projective cylindrical geometry, covering 82% of the solid angle. The remaining crystals are rectangular, and are oriented axially in two end caps, overlapping in solid angle with the ends of the barrel. The barrel region of the calorimeter achieves energy and angular resolutions for electromagnetically showing particles of $\sigma_E/E(\%) = 0.35/E^{0.75} + 1.9 - 0.1E$ and $\sigma_\phi(\text{mrad}) = 2.8/\sqrt{E} + 2.5$ (E in GeV), respectively. The resulting photon energy and direction information provided by this system is used to reconstruct $\eta \rightarrow \gamma\gamma$ decays to determine our η sample size as described below. The crystals are also used in distinguishing electrons from pions. When combined with the tracking and dE/dx information from the drift chambers, the misidentification of pions is limited to less than 1%.

We used 3.11 fb^{-1} of data at the $Y(4S)$ resonance, 10.57 GeV, and 1.69 fb^{-1} of data below the $Y(4S)$ resonance at 10.53 GeV. The samples of on resonance and off resonance hadronic events were

$$N_{\text{had}}(\text{on}) = 1.78 \times 10^7, \quad (11)$$

$$N_{\text{had}}(\text{off}) = 0.797 \times 10^7. \quad (12)$$

We note that 75% of the on resonance events are of the same type as the off resonance (also called continuum) events. The remaining 25% of the on resonance events are from $e^+ e^- \rightarrow B\bar{B}$ production. We found that a major source

of contamination in the search for $\eta \rightarrow e^+e^-$ decay is one real electron from the semileptonic decay of the B or \bar{B} plus one false electron from a pion from the \bar{B} or B decay chain. We substantially reduce the number of $B\bar{B}$ events by applying the following selection criterion to the on resonance events. We require $R_2 \geq 0.3$, where $R_2 \equiv H_2/H_0$ and H_0, H_2 are the zeroth and second Fox-Wolfram moments, respectively [7]. This selectively removes almost all of the more spherically shaped events (see the Appendix for clarification). Thus when discussing our total sample size, we emphasize the number of continuum events in our data sample:

$$N_{\text{had}}(\text{on}) = 1.34 \times 10^7, \quad (13)$$

$$N_{\text{had}}(\text{off}) = 0.797 \times 10^7. \quad (14)$$

Note that this requirement also removes about 50% of the more collimated continuum events; this effect is included in the efficiencies we determine below.

We determined the number of η mesons in the events in Eqs. (13) and (14) using the following procedure. We selected pairs of photons from the decay

$$\eta \rightarrow \gamma\gamma. \quad (15)$$

We then used continuum $e^+e^- \rightarrow$ hadron events generated from Monte Carlo [8] and our simulation of the properties of the CLEO II detector to determine the efficiency for detecting $\eta \rightarrow \gamma\gamma$. We also calculated the average number of η 's produced per event. We now give the details of the procedure.

B. Observed $\eta \rightarrow \gamma\gamma$ decays

In developing the criteria for selecting photon pairs from $\eta \rightarrow \gamma\gamma$ we kept in mind that we would be looking for $\eta \rightarrow e^+e^-$. As much as possible we chose the same selection criteria for γ pairs as we would use for the e^+e^- pairs. In this way any uncertainties in the Monte Carlo modeling of the events will be applied to both decays and thus cancel out of the analysis. For example, since a crucial identification signal for both γ 's and e 's is an electromagnetic shower in the calorimeter, and since a minimum shower energy of 0.4 GeV is required for precise $e-\pi$ separation, we set the minimum shower energy at 0.4 GeV for γ 's as well.

Only $e^+e^- \rightarrow$ hadron events were used by requiring the following selection criteria. First, the events must have at least five charged tracks each of momentum greater than 225 MeV/c. Second, nonannihilation events such as those from beam-gas or beam-wall interactions were rejected. Third, for events taken at beam energies corresponding to the $\Upsilon(4S)$ resonance, $B\bar{B}$ events were removed by the R_2 cut described previously. Further selection criteria for identifying γ 's from $\eta \rightarrow \gamma\gamma$ were the following.

(a) The electromagnetic shower must occur in the main (barrel) portion of the electromagnetic calorimeter. Specifically, $|\cos\theta| < 0.71$ where θ is the angle between the γ direction and the beam axis.

(b) The angle between the shower and the nearest charged particle track must be larger than 20° .

(c) The shower energy must be larger than 0.4 GeV.

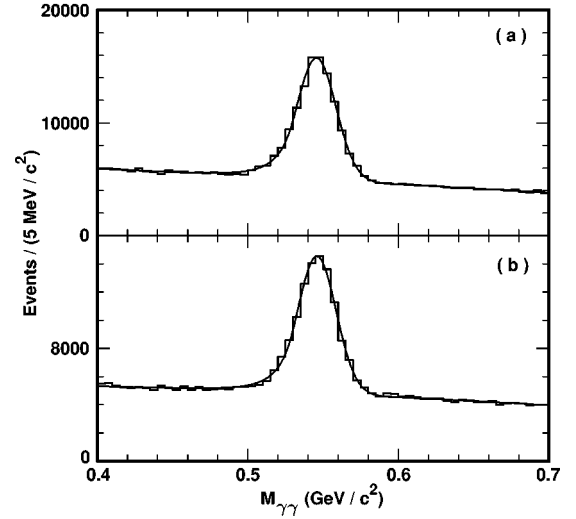


FIG. 2. Measured γ pair invariant mass distribution for (a) on resonance events and (b) off resonance events.

(d) The pattern of energy deposition of the shower in the crystals must be characteristic of a single photon (two or more clusters of deposited energy indicate randomly overlapping photons or a high-momentum π^0).

(e) The shower must not appear to be a fragment from another shower or from a charged pion interaction.

(f) If two γ 's have an invariant mass within 2.5σ ($12.5 \text{ MeV}/c^2$) of the π^0 mass, both γ 's were discarded.

Using γ 's selected with these six criteria we then considered all combinations of pairs subject to the condition that

$$|\mathbf{p}_1 + \mathbf{p}_2| > 0.8 \text{ GeV}/c, \quad (16)$$

where \mathbf{p}_1 and \mathbf{p}_2 are the vector momenta of the two γ 's. We set this condition to reduce the number of random pairings of γ 's.

Figure 2 shows the invariant mass spectra for γ pairs for the on and off resonance data. The η mass peaks at $546 \text{ MeV}/c^2$ have the widths expected from the properties of the CLEO II detector, namely $\sigma = 12.8 \text{ MeV}/c^2$. Fits to these spectra gave the following number of observed $\eta \rightarrow \gamma\gamma$ decays:

$$N_{\eta \rightarrow \gamma\gamma}(\text{on}) = (7.59 \pm 0.12) \times 10^4, \quad (17)$$

$$N_{\eta \rightarrow \gamma\gamma}(\text{off}) = (6.57 \pm 0.06) \times 10^4. \quad (18)$$

Hence we observed about 1.42×10^5 $\eta \rightarrow \gamma\gamma$ decays.

C. Efficiency for detecting $\eta \rightarrow \gamma\gamma$

In determining the efficiency for detecting $\eta \rightarrow \gamma\gamma$ events we restricted ourselves to simulated $e^+e^- \rightarrow$ hadron events in the continuum. Using the selection criteria described in Secs. III A and III B and the known number of η 's in our Monte Carlo sample, we calculated the efficiency for on resonance (with the R_2 cut) and off resonance (without the R_2 cut). Since from Eqs. (13) and (14) we see that 37.5% of our events are off resonance and 62.5% of our events are on resonance, we use these fractions to find a weighted mean efficiency for $\eta \rightarrow \gamma\gamma$,

$$\varepsilon_{\eta \rightarrow \gamma\gamma} = (4.80 \pm 0.05)\% \quad (19)$$

where the error is statistical. The systematic error, which is substantially larger, will be discussed in Sec. V. We also found good agreement between the observed $\eta \rightarrow \gamma\gamma$ events and the simulated $\eta \rightarrow \gamma\gamma$ events with respect to the η momentum spectrum, the η angular distribution, and the γ pair invariant mass distribution of both the η peak and the background.

One major reason for the small efficiency in Eq. (19) is that the η momentum, p_η , is required to be larger than 0.8 GeV/c, but most η 's are produced at smaller momenta. Also responsible for the small efficiency is the requirement that the γ shower energy in the calorimeter, E_γ , be greater than 0.4 GeV. Smaller lower limits on p_η and E_γ would increase $\varepsilon_{\eta \rightarrow \gamma\gamma}$ substantially, but would result in large increases in background for $\eta \rightarrow e^+e^-$.

IV. SEARCH FOR $\eta \rightarrow e^+e^-$ DECAYS

As already noted we limited our systematic uncertainties, particularly our dependence on simulated event sets, by using as much as possible the same selection criteria for $\eta \rightarrow e^+e^-$ events as we used for the observed $\eta \rightarrow \gamma\gamma$ events, Secs. III B and III C.

Beginning with the same event sample in Eqs. (13) and (14) we again require five charged tracks, classification as an annihilation event, and $R_2 > 0.3$ for the on resonance events. We then looked for showers associated with a charged track which met the following criteria: (a) the shower angle θ must satisfy $|\cos\theta| < 0.71$; (b) the shower energy must be larger than 0.4 GeV; (c) the energy deposition of the shower in the crystals must be characteristic of a single photon; (d) the shower must not appear to be a fragment from another shower or from a charged pion interaction; (e) we require $|\mathbf{p}_1 + \mathbf{p}_2| > 0.8$ GeV/c.

The charged particle track had to satisfy our standard criteria for a track from the primary interaction vertex, namely: (f) the track had to be of good quality, as identified by the CLEO software tracking algorithms; (g) the distance of closest approach of the track to the beam line had to be less than 5 mm; (h) the distance of closest approach of the track to the event vertex measured parallel to the beam line had to be less than 50 mm.

Next the track had to be identified as an electron using a standard CLEO algorithm combining E/p , shower shape, and several other parameters. The algorithm has an efficiency of greater than 90%, with the exact efficiency depending on \mathbf{p}_e , and a fake rate from charged pions of about 0.5%.

We then calculated the invariant mass of every e^+e^- combination in the events of Eqs. (13) and (14). Figure 3 shows the spectrum in the mass range of 0.5 to 0.6 GeV/c². There is no peak at the η mass of 547 MeV/c². A study of simulated $\eta \rightarrow e^+e^-$ decays showed that a peak would have a σ of about 5 MeV/c².

V. CALCULATION OF UPPER LIMIT, ERRORS, AND FINAL REMARKS

A. Calculation of upper limit on $B(\eta \rightarrow e^+e^-)$ and errors

To determine the upper limit on the branching fraction $B(\eta \rightarrow e^+e^-)$ we have to know the efficiency for the detec-

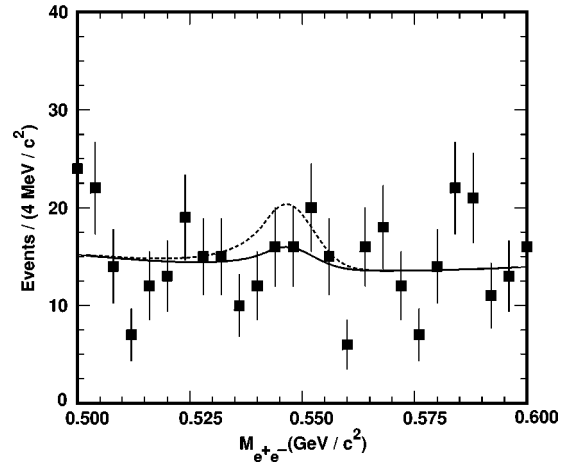


FIG. 3. Invariant mass spectrum of e^+e^- pairs found in the search for $\eta \rightarrow e^+e^-$ decays. There is no peak at the η mass of 0.547 GeV/c². The dashed curve shows the 90% upper limit for the $\eta \rightarrow e^+e^-$ signal plus background.

tion of $\eta \rightarrow e^+e^-$ decays using the criteria in Sec. IV. We generated simulated $\eta \rightarrow e^+e^-$ decays, applied these criteria and found the total efficiency by taking a weighted mean of on resonance and off resonance data as in Sec. III C. The mean efficiency was found to be

$$\varepsilon'_{\eta \rightarrow e^+e^-} = (5.22 \pm 0.31)\%, \quad (20)$$

where the error is statistical.

We used the same simulated events to parametrize the shape of a hypothetical $\eta \rightarrow e^+e^-$ peak, resulting in a mass of (545.9 ± 0.1) MeV/c² and a width (σ) of (5.4 ± 0.1) MeV/c², where the errors are statistical. This shape was then used to fit the data of Fig. 3 to find a 90% confidence upper limit on the number of $\eta \rightarrow e^+e^-$ decays, $N_{\eta \rightarrow e^+e^-}$. Varying the mean and σ of the fit by one standard deviation, and alternately applying linear and quadratic background functions, gave a range of values for $N_{\eta \rightarrow e^+e^-}$ from 18.4 to 27.1 events. We used the most conservative of these fits and concluded

$$N_{\eta \rightarrow e^+e^-} < 27.1. \quad (21)$$

It is at this point that we must consider the major sources of systematic error in our analysis. As we have already minimized the uncertainty from the electromagnetic calorimeter selection criteria, our remaining sources of systematic error stem from our tracking, particle identification, and photon detection efficiencies, as well as the uncertainties in $N_{\eta \rightarrow \gamma\gamma}$, $\varepsilon_{\eta \rightarrow \gamma\gamma}$, $\varepsilon'_{\eta \rightarrow e^+e^-}$, and $B(\eta \rightarrow \gamma\gamma)$. The total systematic uncertainty of 10.7% is calculated in Table I. In our final calculation we reduce our mean efficiency by this amount, yielding

$$\varepsilon_{\eta \rightarrow e^+e^-} = 4.66\%. \quad (22)$$

Finally, we normalize to the branching fraction of $\eta \rightarrow \gamma\gamma$,

TABLE I. Summary of systematic uncertainty.

Source	Uncertainty
Tracking efficiency	1% per e candidate
Electron ID efficiency	3% per electron
Photon detection efficiency	3% per photon
$N_{\eta \rightarrow \gamma\gamma}$ (stat.)	1.4%
$\varepsilon_{\eta \rightarrow \gamma\gamma}$ (stat.)	1.0%
$\varepsilon_{\eta \rightarrow e^+e^-}$ (stat.)	6.0%
$B(\eta \rightarrow \gamma\gamma)$	0.7%
Total	10.7%

$$B(\eta \rightarrow e^+e^-) = \frac{N_{\eta \rightarrow e^+e^-}}{N_{\eta \rightarrow \gamma\gamma}} \frac{\varepsilon_{\eta \rightarrow \gamma\gamma}}{\varepsilon_{\eta \rightarrow e^+e^-}} B(\eta \rightarrow \gamma\gamma) \quad (23)$$

and arrive at our 90% confidence upper limit,

$$B(\eta \rightarrow e^+e^-) < 7.7 \times 10^{-5}. \quad (24)$$

This upper limit is indicated by the dashed curve in Fig. 3.

B. Final remarks

Our limit of $B(\eta \rightarrow e^+e^-) < 7.7 \times 10^{-5}$ agrees with and improves upon the upper limit of 2×10^{-4} found by White *et al.* [9]; both of the confidence levels are 90%. White *et al.* used the reaction $p + d \rightarrow {}^3\text{He} + \eta$ to produce η 's combined with a two-arm counter telescope to search for the $\eta \rightarrow e^+e^-$ decay. In the course of concluding our analysis we have considered if improvements could be made in our method.

We note from Eqs. (17) and (18) that about 1.4×10^5 $\eta \rightarrow \gamma\gamma$ events were observed. Since $\varepsilon_{\eta \rightarrow \gamma\gamma}$ and $\varepsilon_{\eta \rightarrow e^+e^-}$ are about the same, we should have been able to investigate a $B(\eta \rightarrow e^+e^-)$ of the order

$$B(\eta \rightarrow e^+e^-) \sim \left(\frac{2.3}{1.4 \times 10^5} \right) B(\eta \rightarrow \gamma\gamma) \sim 6 \times 10^{-6} \quad (25)$$

if there were no background events. In the future when the number of detected $e^+e^- \rightarrow$ hadron events increase twofold or more at CESR, and at the B factories now under construction, one might hope to achieve a sensitivity of 10^{-6} .

However there is a background primarily from pairs containing one true electron and one pion misidentified as an electron. Removing $B\bar{B}$ decays aided us somewhat, but unless this background is further reduced, sensitivities of 10^{-5} to 10^{-6} for $B(\eta \rightarrow e^+e^-)$ cannot be achieved by our method. The RICH detector that will be installed for CLEO III should help improve the pion-electron separation. In addition, substantial improvement in sensitivity will probably be achieved using fixed target η production via hadronic collisions and specially designed electronic detectors.

ACKNOWLEDGMENTS

We gratefully acknowledge the effort of the CESR staff in providing us with excellent luminosity and running conditions. J.P.A., J.R.P., and I.P.J.S. thank the NYI program of the NSF; M.S. thanks the PFF program of the NSF; G.E. thanks the Heisenberg Foundation; K.K.G., M.S., H.N.N., T.S., and H.Y. thank the OJI program of U.S. DOE; J.R.P., K.H., M.S., and V.S. thank the A.P. Sloan Foundation; A.W. and R.W. thank the Alexander von Humboldt Stiftung; and M.S. thanks Research Corporation for support.

APPENDIX: VALIDITY OF SUPPRESSING $B\bar{B}$

Our efficiencies for the on resonance and off resonance searches for $\eta \rightarrow \gamma\gamma$, i.e., with and without the R_2 cut, respectively, are

$$\varepsilon_{\eta \rightarrow \gamma\gamma}(\text{on}) = (3.75 \pm 0.05)\%, \quad (A1)$$

$$\varepsilon_{\eta \rightarrow \gamma\gamma}(\text{off}) = (6.57 \pm 0.07)\%. \quad (A2)$$

Combining Eq. (A2) with the number of events in our off resonance sample [Eq. (14)], the number of η 's observed [Eq. (18)], and $B(\eta \rightarrow \gamma\gamma)$, we find the number of η 's produced per continuum event to be

$$n_{\eta}(\text{cont}) = 0.315 \pm 0.006. \quad (A3)$$

Multiplying this result by the number of on resonance continuum events [Eq. (13)], the on resonance efficiency [Eq. (A1)], and $B(\eta \rightarrow \gamma\gamma)$ gives the number of $\eta \rightarrow \gamma\gamma$ decays we should expect to see from on resonance continuum events:

$$N_{\eta \rightarrow \gamma\gamma}(\text{on}) = (6.50 \pm 0.25) \times 10^4. \quad (A4)$$

Subtracting this from the number of decays we do see, Eq. [(17)], this leaves about $10\,900 \pm 2800$ $\eta \rightarrow \gamma\gamma$ decays that must come from $B\bar{B}$ events, or about $(8 \pm 2)\%$ of the total number of on and off resonance decays we observe. Thus it seems that our assumption that all $B\bar{B}$ events are suppressed leads to a small overestimate of $N_{\eta \rightarrow \gamma\gamma}$.

However, one must remember that $N_{\eta \rightarrow \gamma\gamma}$ and $N_{\eta \rightarrow e^+e^-}$ will have almost equal proportional contributions from $B\bar{B}$ events. In fact the only discrepancy between the two contributions will be due to slightly different acceptances, caused by the differing angular and momentum distributions of the two channels. Since in calculating our final limit we take the ratio $N_{\eta \rightarrow e^+e^-}/N_{\eta \rightarrow \gamma\gamma}$, the $B\bar{B}$ contributions will almost entirely cancel. The remaining effect will be much smaller than 8%, and thus negligible for an upper limit.

- [1] L. Bergström, Z. Phys. C **14**, 129 (1982).
- [2] L. G. Landsberg, Phys. Rep. **128**, 301 (1985).
- [3] *Review of Particle Physics*, R. M. Barnett *et al.*, Phys. Rev. D **54**, 1 (1996).
- [4] R. S. Kessler *et al.*, Phys. Rev. Lett. **70**, 892 (1993).
- [5] R. I. Dzholyadin *et al.*, Phys. Lett. **97B**, 471 (1980).
- [6] CLEO Collaboration, Y. Kubota *et al.*, Nucl. Instrum. Methods Phys. Res. A **320**, 66 (1992).
- [7] G. Fox and S. Wolfram, Phys. Rev. Lett. **41**, 1581 (1978).
- [8] JETSET 7.3: T. Sjöstrand and M. Bengtsson, Comput. Phys. Commun. **43**, 367 (1987).
- [9] D. B. White *et al.*, Phys. Rev. D **53**, 6658 (1996).